

Mesenchymal Stem/Stromal Cells Derived From a Reproductive Tissue Niche Under Oxidative Stress Have High Aldehyde Dehydrogenase Activity

Gina D. Kusuma^{1,2} · Mohamed H. Abumaree³ · Mark D. Pertile^{4,5} · Anthony V. Perkins⁶ · Shaun P. Brennecke^{1,2} · Bill Kalionis^{1,2}

Published online: 15 February 2016
© Springer Science+Business Media New York 2016

Abstract The use of mesenchymal stem/stromal cells (MSC) in regenerative medicine often requires MSC to function in environments of high oxidative stress. Human pregnancy is a condition where the mother's tissues, and in particular her circulatory system, are exposed to increased levels of oxidative stress. MSC in the maternal *decidua basalis* (DMSC) are in a vascular niche, and thus would be exposed to oxidative stress products in the maternal circulation. Aldehyde dehydrogenases (ALDH) are a large family of enzymes which detoxify aldehydes and thereby protect stem cells against oxidative damage. A subpopulation of MSC express high levels of ALDH (ALDH^{br}) and these are more potent in repairing and regenerating tissues. DMSC was compared with chorionic villous MSC (CMSC) derived from the human placenta.

CMSC reside in vascular niche and are exposed to the fetal circulation, which is in lower oxidative state. We screened an ALDH isozyme cDNA array and determined that relative to CMSC, DMSC expressed high levels of ALDH1 family members, predominantly ALDH1A1. Immunocytochemistry gave qualitative confirmation at the protein level. Immunofluorescence detected ALDH1 immunoreactivity in the DMSC and CMSC vascular niche. The percentage of ALDH^{br} cells was calculated by Aldefluor assay and DMSC showed a significantly higher percentage of ALDH^{br} cells than CMSC. Finally, flow sorted ALDH^{br} cells were functionally potent in colony forming unit assays. DMSC, which are derived from pregnancy tissues that are naturally exposed to high levels of oxidative stress, may be better candidates for regenerative therapies where MSC must function in high oxidative stress environments.

✉ Bill Kalionis
Bill.kalionis@thewomens.org.au

¹ Department of Obstetrics and Gynaecology, University of Melbourne, Royal Women's Hospital, Parkville, VIC 3052, Australia

² Pregnancy Research Centre, Department of Maternal-Fetal Medicine, Royal Women's Hospital, Parkville, VIC 3052, Australia

³ King Abdullah International Medical Research Center/ King Saud Bin Abdulaziz University for Health Sciences, College of Science and Health Professions, King Abdulaziz Medical City – National Guard Health Affairs, P.O. Box 3660, Riyadh 11481 Mail Code 3124, Kingdom of Saudi Arabia

⁴ Victorian Clinical Genetics Services, Murdoch Children's Research Institute, Royal Children's Hospital, Flemington Road, Parkville, VIC 3052, Australia

⁵ Department of Paediatrics, University of Melbourne, Royal Children's Hospital, Parkville, VIC 3052, Australia

⁶ School of Medical Science, Menzies Health Institute Queensland, Griffith University, Gold Coast Campus, Southport, QLD 9726, Australia

Keywords Mesenchymal stem cells · Chorionic villi · Decidua · Placenta · Aldehyde dehydrogenase

Introduction

Mesenchymal stem/stromal cells (MSC) have generated much interest as a potential source for cell-based therapeutic strategies due to their immunosuppressive, anti-inflammatory, and detoxification properties [1–3]. The use of MSC in regenerative medicine often requires MSC to function in environments of high oxidative stress or to treat oxidative stress-related pathologies such as stroke/ischemia, diabetes, Parkinson's disease, and acute myocardial infarction [4–6]. However, MSC used for these purposes are often sourced from tissues that are not normally exposed to increased oxidative stress. Oxidative stress can significantly affect MSC properties and strategies have been developed to pre-condition MSC to hypoxia, which

can improve MSC proliferation and differentiation [7]. Our alternative approach is to source MSC from tissues that are naturally exposed to high levels of oxidative stress.

Human pregnancy is a condition where the mother's tissues, and in particular her circulatory system, are exposed to increased levels of oxidative stress. In comparison to the postpartum period, high levels of reactive oxygen species (ROS) during embryonic, fetal and placental development are features of uncomplicated human pregnancies [8, 9]. The maternal-placental interface, which comprises of fetal villous tissue derived from the chorionic sac, and maternal *decidua basalis*, are abundant sources of MSC. Our previous studies showed the niche of chorionic MSC (CMSC) and *decidua basalis* MSC (DMSC) is vascular [10, 11]. Based on their niche within the maternal-placental interface, DMSC and CMSC are likely to be exposed to different levels of oxidative stress. DMSC are in close proximity to endothelial cells of the maternal vessels, which are in direct contact with the maternal blood circulation and exposed to ROS such as lipid peroxides, malondialdehyde, peroxynitrite, and nitric oxide [9, 12–14]. On the other hand, CMSC are in close contact with the fetal blood circulation, which is in a lower oxidative state [15].

One of the most important families of enzymes that impart resistance to oxidative stress on MSCs is the aldehyde dehydrogenase (ALDH family). High ALDH activity is one of the attributes of many stem cells and contributes significantly to cell survival, i.e. the ability to eliminate toxic and xenobiotic aldehydes in humans [16–19]. ALDH enzymes are of particular interest in stem cell research because they are involved in a variety of important stem cell functions including regulation of self-renewal ability, differentiation potential, and oxidative stress response [17].

High ALDH activity is an alternative method of identifying stem cells and is considered to be one of few “universal” stem cell markers [19, 20]. High ALDH activity is characteristic of stem cells isolated from human umbilical cord blood, bone marrow, brain, cornea, lens, skeletal muscle, adipose tissue, and the gastrointestinal tract [17, 19, 21–24]. The means for ALDH detection are diverse (immunohistochemistry, Western blotting, FACS and fluorescence microscopy), making it a powerful tool for stem cell detection and characterization in many tissues. The most popular and commercially available technique in measuring ALDH enzyme activity in cells is a method based on the fluorescent substrate BODIPY aminoacetaldehyde (BAAA), also known as the Aldefluor assay [25]. The Aldefluor assay detects ALDH activity by flow cytometry and the subpopulation of cells with high ALDH activity is referred to as ALDH^{br} cell population. Aldefluor-stained cells are viable and cell sorting based on Aldefluor staining can be subsequently utilized in experimental protocols in vitro and in vivo [20].

In particular, the ALDH1A1 isozyme is the main cytosolic enzyme responsible for oxidizing a variety of intracellular

aldehydes into carboxylic acids [18]. Various studies have reported that different ALDH isozymes such as ALDH1A1, ALDH1A2, ALDH1B1, ALDH2, ALDH3A1, and ALDH3B1 isozymes might be involved in cytoprotective effects [26]. Although the ALDH1A1 isozyme was first implicated as a characteristic feature of stem cells, it is possible that ALDH activity may be due to the expression of other isozymes. For instance, both ALDH1A1 and ALDH3A1 isozymes are highly expressed in breast and lung cancer stem cells and they contribute to the onset of drug resistance in these cells [17, 25].

We used the human placenta as a model organ to study the expression of ALDH enzyme in MSC that reside in niches exposed to differing levels of oxidative stress. The first aim of this study was to determine if cultured CMSC and DMSC express the ALDH family of enzymes and screen for the most highly expressed isozyme. The second aim of this study was to determine if ALDH expression co-localizes with MSC marker in the chorionic villi and *decidua basalis* using multi-label immunofluorescence on the basal plate of placenta. A combination of ALDH1 and FZD-9 antibodies as stem cells markers were used in conjunction with vWF as an endothelial cell marker. The final aim was to compare the ALDH levels in CMSC and DMSC, which represent MSC from niches exposed to different level of oxidative stress in the placenta. Immunocytochemistry, real-time RT-PCR, and the Aldefluor assay were each employed to measure ALDH enzyme activity between different cell populations. Cell sorting based on ALDH activity assisted in isolating each subpopulation of ALDH^{br} and ALDH^{dim} cells. The colony forming unit-fibroblast (CFU-F) assay was carried out to investigate the difference in the cloning efficiency between sorted cell populations.

Materials and Methods

Isolation of CMSC and DMSC

Human term placentae ($n = 13$) were obtained following informed, written patient consent and with the approval of the Human Research and Ethics Committee of the Royal Women's Hospital, Victoria, Australia. The placentae were obtained from healthy women with uncomplicated pregnancies following elective Caesarean section or normal vaginal delivery. Previous studies from this laboratory have shown that mode of delivery is not a significant variable in the study of MSC [10, 27]. CMSC were isolated using our previously published explant method [10, 28, 29]. Briefly, chorionic villous tissue was carefully dissected under a microscope and non-villous tissue removed. Villi were minced into small pieces (1mm³) and digested in 0.25 % trypsin for 40 min at 37 °C. CMSC were cultured in Amniomax C100 complete

medium (Life Technologies, CA, USA) and maintained at 37 °C in a humidified 5 % CO₂ incubator. DMSC were prepared from *decidua basalis* tissue that remained attached to the maternal side of the placenta. *Decidua basalis* tissue was dissected from the surface of a central cotyledon on the maternal side of the placenta as described elsewhere [29, 30]. Briefly, tissues were enzymatically digested and then the cells were fractionated by gradient centrifugation. DMSC were cultured in α -MEM complete medium (Sigma-Aldrich, St Louis, USA) with 10 % FBS, penicillin/streptomycin (100 U/mL and 100 mg/mL, Life Technologies) and 2 mM L-glutamine (Life Technologies).

To further validate the findings, in addition to primary CMSC and DMSC, we utilized the representative cell lines to alleviate the patient-to-patient variation, reproducibility, and cell expansion challenges generally encountered with primary cells. CMSC29 and DMSC23 cell lines were created by human telomerase reverse transcriptase (hTERT) transformation of the CMSC and DMSC populations respectively [31]. In this study, CMSC and DMSC were used up to passage P5 while the transformed cell lines CMSC29 and DMSC23 were used up to passage P25. All cell cultures were maintained at 37 °C in a humidified 5 % CO₂ incubator.

Flow Cytometry, Fluorescence in situ Hybridization (FISH) Analysis, and in vitro Cell Differentiation

MSC surface markers were analyzed on BD LSRII flow cytometer for the following positive markers: CD73, CD105, CD90, CD146, CD44, CD66 and negative markers: CD45, CD19, and HLA-DR. FISH analysis was performed to confirm the maternal or fetal origin of primary CMSC and DMSC. Details of the methodology were described previously [29, 30]. The multi-lineage differentiation potential of isolated MSCs and cell lines was determined by inducing cells with adipogenic, osteogenic, and chondrogenic supplements added to the growth medium as described in detail elsewhere [29, 30].

Taqman cDNA Array for ALDH Isozymes Screening

ALDH isozyme mRNA screening was carried out on CMSC and DMSC. For each primary MSC type, five individual patient placentae from uncomplicated pregnancies were collected. RNA extraction employed the Purelink RNA kit (Life Technologies) and was carried out according to the manufacturer's instructions. Following RNA extraction, a two-step reverse transcription (RT) PCR method was performed. Firstly, cDNA was synthesised from 2 μ g RNA with 500 ng random primers and 0.5 mM of dNTP mix followed by incubation for 5 mins at 65 °C. Subsequently, 1 μ L DTT, 40 U RNasin Plus RNase inhibitor (Promega, WI, USA), 200 U of

Superscript III reverse transcriptase (Life Technologies), and 4 μ L of 5 \times First Strand Buffer was added to each sample. The samples were placed in the GeneAmp PCR system 9700 using the following cycling conditions: 25 °C for 5 mins, 50 °C for 60 mins, and 70 °C for 15 mins. All cDNA samples (2 ng/ μ L) were stored at –20 °C.

Pooled cDNA samples from 5 normotensive pregnancies were used in custom made Taqman array plates prepared by Applied Biosystems (CA, USA). The plate contained primers for 15 known ALDH isozymes as well as the 18S rRNA endogenous control gene (see Table 1). The PCR reaction was performed with 1 μ L pooled cDNA (12.5 ng), 10 μ L Taqman Universal PCR Mastermix No AmpErase UNG, and 9 μ L of distilled water to make up the 20 μ L reaction in each well. The reaction was carried out in the ABI 7500 (Applied Biosystems) real-time PCR machine using the following cycling conditions: 10 mins at 95 °C initially, followed by 95 °C for 15 s and 60 °C for 1 min repeated for 40 cycles. Each array on the pooled cDNA sample was carried out in duplicate and each was normalized to endogenous 18S rRNA. The calibrator sample for this experiment was the CMSC. The maximum allowable C_T value was 40. Relative quantification (RQ) value was calculated by the 2^{– $\Delta\Delta$ CT} method [32].

Real-time RT-PCR for ALDH1A1

To independently verify mRNA levels, for the ALDH1A1 isozyme, the PCR reaction was performed with 1 μ L cDNA (12.5 ng), 5 μ L Taqman Universal PCR Mastermix No AmpErase UNG (Life Technologies), 0.5 μ L of the 18S rRNA housekeeping gene (Hs99999901_s1, Applied Biosystems), 0.5 μ L of the target ALDH1A1 probe (Hs00946916_m1, Applied Biosystems) and 3 μ L of distilled water to make up a final 10 μ L duplex reaction volume in each well of a 96 Microamp optical plate (Life Technologies). The ABI 7500 (Applied Biosystems) cycling conditions were 10 mins at 95 °C initially, then 95 °C for 15 s, and 60 °C for 1 min, which was repeated for 40 cycles. RQ value was calculated by the 2^{– $\Delta\Delta$ CT} method [32].

Multiple Immunofluorescence Labelling

Tissue was collected from the *decidua basalis* that remained attached to a central cotyledon on the maternal side of the placenta following delivery. A piece of *decidua basalis* tissue (about 2 cm \times 1 cm \times 1 cm) was excised, snap frozen in Jung tissue freezing medium (Leica, Weitzlar, Germany) and stored in the –80 °C freezer before use. Five μ m frozen transverse sections were cut and transferred onto Superfrost Plus slides (Thermo Scientific, MA, USA). Multiple immunofluorescence labelling was performed by incubating with mouse anti-human ALDH1 (5 μ g/mL, BD Biosciences) in combination with endothelial cell marker rabbit anti-human vWF

Table 1 C_T values from CMSC and DMSC

| Gene | Taqman [®] gene expression assay number | DMSC | CMSC | log ₂ (RQ) |
|---------|--|---------------------------|--------------|-----------------------|
| ALDH1A1 | Hs00946916_m1 | 26.46 ± 0.01 [#] | 31.40 ± 0.07 | 4.49 ± 0.01 |
| ALDH1A2 | Hs00180254_m1 | 28.58 ± 0.01 | 36.84 ± 0.28 | 7.81 ± 0.01 |
| ALDH1A3 | Hs00167476_m1 | 32.97 ± 0.07 | 29.64 ± 0.04 | -3.78 ± 0.07 |
| ALDH1B1 | Hs00265114_s1 | 26.46 ± 0.03 | 28.57 ± 0.00 | 1.66 ± 0.03 |
| ALDH2 | Hs01007998_m1 | 28.74 ± 0.01 | 28.33 ± 0.02 | -0.87 ± 0.01 |
| ALDH3A1 | Hs00964880_m1 | 36.90 ± 0.12 | 34.75 ± 0.29 | -2.59 ± 0.12 |
| ALDH3A2 | Hs00166066_m1 | 27.39 ± 0.03 | 28.08 ± 0.05 | 0.25 ± 0.03 |
| ALDH3B1 | Hs00997594_m1 | 28.18 ± 0.02 | 28.88 ± 0.01 | 0.25 ± 0.02 |
| ALDH3B2 | Hs02511514_s1 | 35.67 ± 1.22 | 40.00 ± 0.00 | 0.00 ± 0.00 |
| ALDH4A1 | Hs00186689_m1 | 28.86 ± 0.08 | 28.94 ± 0.02 | -0.36 ± 0.08 |
| ALDH5A1 | Hs00542449_m1 | 30.52 ± 0.02 | 31.95 ± 0.06 | 0.98 ± 0.02 |
| ALDH6A1 | Hs00194421_m1 | 28.30 ± 0.02 | 29.51 ± 0.05 | 0.76 ± 0.02 |
| ALDH7A1 | Hs00609622_m1 | 28.05 ± 0.10 | 30.05 ± 0.11 | 1.55 ± 0.10 |
| ALDH8A1 | Hs00988965_m1 | 35.11 ± 0.23 | 34.99 ± 0.08 | -0.56 ± 0.23 |
| ALDH9A1 | Hs00997881_m1 | 26.51 ± 0.09 | 26.93 ± 0.02 | -0.03 ± 0.09 |

[#] C_T values reflect the fractional cycle number at which the fluorescence intensity exceeds the threshold intensity. Data are presented as mean ± SEM

(1 µg/mL, Thermo Scientific), followed by donkey anti-mouse Alexa Fluor 488 (4 µg/mL, Life Technologies) and goat anti-rabbit Alexa Fluor 568 (0.5 µg/mL, Life Technologies) secondary antibodies respectively. On another slide, sections were incubated with mouse anti-human ALDH1 (5 µg/mL) in combination with rabbit anti-human FZD-9 (10 µg/mL, Biologend, CA, USA), followed by donkey anti-mouse Alexa Fluor 488 (4 µg/mL) and goat anti-rabbit Alexa Fluor 568 (20 µg/mL) secondary antibodies respectively. The negative control was the omission of the primary antibodies. Sections were mounted using a fluorescent mounting medium incorporating a DAPI nuclear counterstain (Vectamount). To distinguish between *decidua basalis* and chorionic villous tissues, serial sections were prepared and stained with Haematoxylin and Eosin staining (data not shown). Immunostaining was visualised with a fluorescence microscope (Olympus IX81) with the appropriate filters and the resulting multi-colour image was composited by Cell R software (Olympus).

Immunocytochemistry

Immunocytochemistry was performed with ALDH1 antibody on cultured cells. Cultured cells were seeded and fixed with 70 % ethanol into an 8-well glass chamber slide (BD Biosciences, CA, USA) for immunocytochemistry. To prevent non-specific staining, sections were blocked with 5 % skim milk powder for 1 h at RT and then washed with 1X PBS. ALDH1 expression was determined by staining with mouse anti-human ALDH1 (5 µg/mL, BD Biosciences) followed by Alexa Fluor 488 (20 µg/mL, Life Technologies) secondary antibody [21]. The negative control was omission of the

primary antibody. Nuclear counterstaining was carried out by the addition of Vectashield mounting medium with DAPI (Vector Laboratories, CA, USA). Staining was visualized using an Olympus IX81 microscope with the appropriate fluorescence filters and the resulting multi-colour images were compiled by Cell R software (Olympus).

Aldefluor Assay

The Aldefluor assay kit (Stem Cell Technologies, Vancouver, Canada) was employed to determine the percentage of cells expressing high levels of ALDH, i.e. ALDH^{br} cells [33]. This assay is based on the intracellular metabolism of BAAA (Aldefluor) substrate by ALDH enzyme, which results in the intracellular accumulation of BAA with more intense fluorescence in viable cells that express bright levels of ALDH activity (i.e. ALDH^{br} cells). The remaining MSC that express low levels of ALDH activity are referred to as ALDH^{dim} cells.

For each experiment, 1 × 10⁶ cells were incubated with Aldefluor substrate for 30 mins at 37 °C, with and without the ALDH inhibitor, diethylaminobenzaldehyde (DEAB) according to the manufacturer's instructions. After incubation, cells were washed once with Aldefluor assay buffer containing 1 µg/mL DAPI (Sigma-Aldrich). To achieve a single cell suspension, cells were filtered into a 5 mL tube fitted with a cell strainer cap. Cells were selected for analysis based on their viability and their forward versus side scatter profile. Cells incubated with Aldefluor in the presence of DEAB were used to establish baseline fluorescence. The brightly fluorescent ALDH^{br} cells were detected in the FITC channel on a BD LSR II flow cytometer using FACS Diva software (BD).

For cell sorting, 1×10^7 DMSC23 cells were prepared and stained according to the Aldefluor assay protocol. ALDH^{br} and ALDH^{dim} cells were sorted using a MoFlo cell sorter (Beckman Coulter, CA, USA) and Cyclops SUMMIT software (Cytomation, Inc., CO, USA). Cells were sorted on the basis of their ALDH activity using published methods [34]. After sorting, ALDH^{br} and ALDH^{dim} cells were cultured in 75 cm² tissue culture flasks and allowed to grow until 80 % confluent.

CFU-F Assay

A CFU-F assay was carried out to determine the cloning efficiency of DMSC23 cells following cell sorting based on ALDH activity. A characteristic feature of many types of stem cells is their clonogenicity i.e. the ability of a single cell to produce a colony when seeded at low densities. An accepted definition of a colony is one that contains more than 50 cells. DMSC23 cells, sorted ALDH^{br} DMSC23 cells, and sorted ALDH^{dim} DMSC23 cells were dissociated from the culture flask. The resulting cell suspensions were seeded into 6-well plates at a cell density of 400 cells per well. Plates were incubated for 2 weeks without a medium change. Cells were then briefly rinsed with PBS, fixed with 10 % formalin, and Giemsa stained for visualization. A group of cells containing 50 cells or more, with a defined colony margin, was counted as a colony. The CFU-F result was presented as the % cloning efficiency.

$$\% \text{cloning efficiency} = \frac{\text{number of colony formed}}{400 \text{ cells}} \times 100\%$$

Statistical Analysis

All data from the Aldefluor assay and real-time RT-PCR were described as mean \pm SEM. An unpaired student t-test was used to assess the difference in percentage of ALDH^{br} cells and real-time RT-PCR results between different groups. A *p*-value of <0.05 was considered significant. Statistical calculations were performed using the GraphPad Prism software.

Results

Isolation and Characterization of CMSC and DMSC

Figure 1a, b shows the fetal and maternal origin of the respective CMSC and DMSC populations. Isolated CMSC and DMSC at passage P1 adhere to plastic and showed the uniform fibroblast-like morphology typical of MSCs (Fig. 1c, d). Culture conditions for CMSC included the use of Amniomax

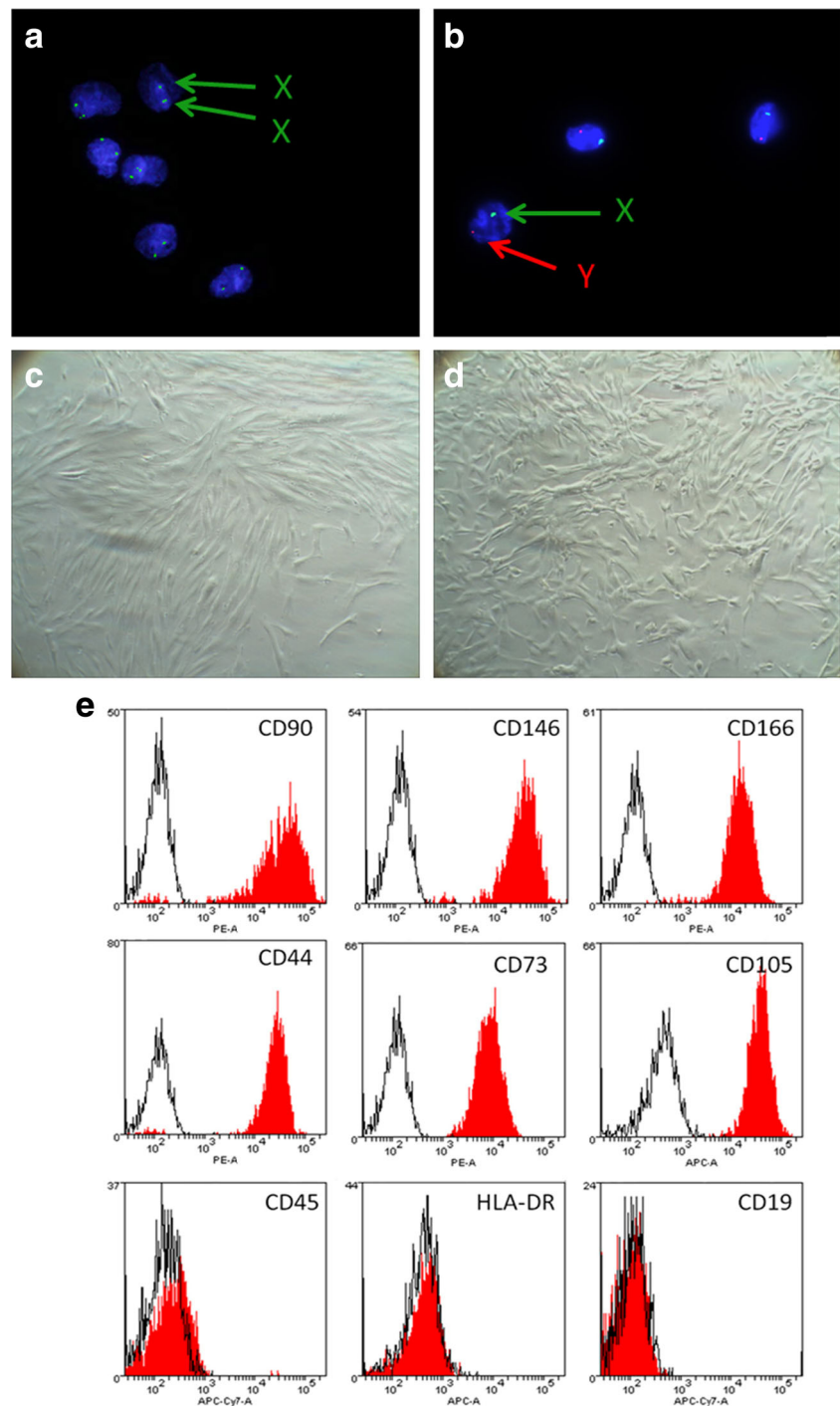
complete medium and DMSC in α -MEM basal medium with 10 % FCS. Figure 1e illustrates the cell surface marker profile for DMSC with the typical positive expression of CD90, CD146, CD166, CD44, CD73, and CD105; as well as negative expression of CD45, CD19, and HLA-DR. CMSC expressed a similar cell surface marker profile to DMSC (data not shown). Figure 2a–c shows DMSC differentiation into cells of the osteogenic, adipogenic, and chondrogenic lineages. Differentiation of CMSC was found to be similar (data not shown). Undifferentiated cells only show background staining (Fig. 2d–f).

Taqman cDNA Array Screening of ALDH Isozymes

A custom Taqman cDNA array was used to compare the mRNA levels of different ALDH isozymes between CMSC and DMSC. The real-time RT-PCR reactions were run for 40 cycles using universal cycling conditions. The mRNA level of each ALDH isozyme was normalized to the housekeeping gene 18S rRNA. The threshold cycle or C_T values are presented in Table 1. CMSC and DMSC expressed different levels of mRNA for the various ALDH isozymes. C_T values of low numerical values (<30) indicate strong positive reactions correlated to relative abundance of mRNA transcript in the sample. On the other hand, C_T values of high numerical values (>30) suggested that the mRNA transcript in that sample was at a relatively low level. In DMSC, mRNA levels of ALDH1A1 (26.46 ± 0.01), ALDH1B1 (26.46 ± 0.03), and ALDH9A1 (26.51 ± 0.09) isozymes were the highest. The ALDH3B2 isozyme mRNA was only detected in DMSC. In CMSC, ALDH9A1 (26.93 ± 0.02) mRNA levels were highest, followed by ALDH3A2 (28.08 ± 0.05) and ALDH2 (28.33 ± 0.02). Overall, the results show that, in addition to the ALDH1A1 isozyme, these cells expressed mRNA for several ALDH genes from other families.

To determine the relative mRNA levels of ALDH isozymes in CMSC and DMSC, $\log_2(\text{RQ})$ values or fold change were calculated and plotted in the Y-axis against the target genes in the X-axis (Fig. 3a). CMSC were used as the calibrator sample for the fold change calculation. For the analysis presented in Fig. 3a, ALDH3B2 isozyme in CMSC sample was assigned a C_T value of 40 even though the sample did not produce sufficient fluorescence to cross the threshold of detection. Genes in DMSC with relative mRNA levels of more than a two-fold increase relative to CMSC were classified as up-regulated and conversely, genes in DMSC with relative mRNA levels of more than two-fold decrease relative to CMSC were classified as down-regulated. ALDH1A1 and ALDH1A2 isozymes showed the greatest fold increases of 4.49 and 7.81 relative to CMSC mRNA levels of these genes, respectively. ALDH1A3 and ALDH3A1 isozymes showed the greatest fold decreases of -3.78 and -2.60 relative to CMSC mRNA levels for these genes, respectively. Other ALDH isozymes

Fig. 1 Characterization of cultured DMSC and CMSC. Representative FISH analysis carried out on cells isolated from placenta of male newborn **(a)** DMSC showed two X chromosomes (Spectrum Green) signals, **(b)** CMSC showed one X chromosome (Spectrum Green) and one Y chromosome (Spectrum Orange) signals. Cell nuclei were stained blue with DAPI. Magnification is 1000 \times . Bright field microscopy image of **(c)** DMSC cells at P1 **(d)** CMSC cells at P1. Magnification is 100 \times and scalebar is 100 μ m. DMSC cell surface marker expression **(e)**. Histograms showing DMSC positive expression for CD90, CD146, CD166, CD44, CD73, CD105 and negative expression of CD45, CD19, and HLA-DR. The red histogram shows the MSC marker antibody staining while the white histogram shows the matching isotype control antibody staining



(ALDH1B1, ALDH2, ALDH3A2, ALDH3B1, ALDH4A1, ALDH5A1, ALDH6A1, ALDH7A1, ALDH8A1, and ALDH9A1) did not show more than two-fold mRNA level changes in DMSC relative to CMSC.

Real-time RT-PCR

ALDH1A1 mRNA levels in CMSC and DMSC were analyzed relative to 18S rRNA, which was used as the

housekeeping control gene for normalisation. The RQ value was calculated relative to the CMSC samples. Figure 3b shows significantly increased ALDH1A1 mRNA levels in DMSC in comparison to CMSC (DMSC: 5448 ± 1880 vs. CMSC: 0.99 ± 0.03 , p -value = 0.0274, $n = 6$, unpaired t -test).

The ALDH1A1 mRNA levels were further analyzed in CMSC29 and DMSC23 cells. RQ value was calculated relative to the CMSC29 cells samples. Figure 3c shows a

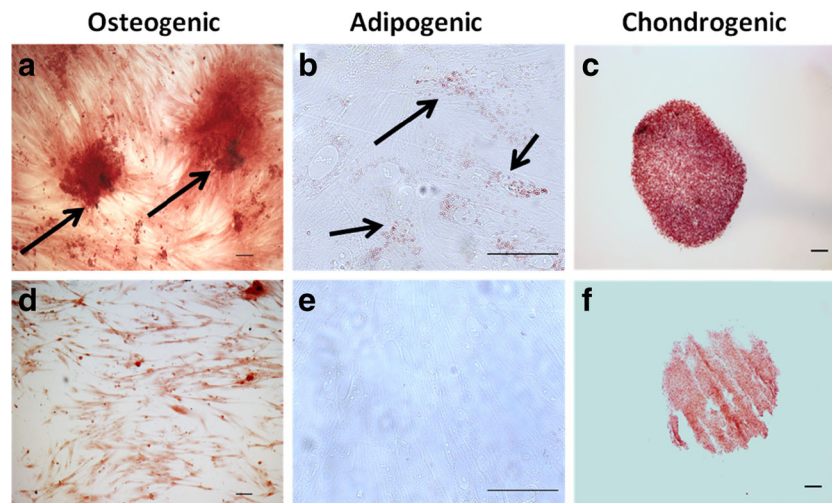


Fig. 2 DMSC differentiation into mesenchymal lineages. **(a)** Osteogenic differentiation, Alizarin Red staining in cells after 5 weeks growth in osteogenic induction medium. Arrows show calcium depositions. **(b)** Adipogenic differentiation, Oil Red O staining in cells after 14 days growth in adipogenic induction medium. Arrows show fat droplets. **(c)**

Chondrogenic differentiation, Safranin O staining for proteoglycans depositions in cells after 21 days growth in chondrogenic induction medium. **(d-f)** Control uninduced DMSC in media without differentiation supplements. Scalebar is 100 μm

significantly increased ALDH1A1 mRNA levels in the DMSC23 cells compared to the CMSC29 cells (DMSC23: 4239 ± 131.1 vs. CMSC29: 0.98 ± 0.15 , p -value <0.001 , $n = 5$, unpaired t-test).

Multiple Immunofluorescence Labelling with ALDH1 Antibody

Multiple immunofluorescence labelling was conducted to localize the immunoreactivity of the ALDH1 antibody within the chorionic villi and *decidua basalis* of the human term placenta. The reactions were carried out with sections prepared from at least 3 different placenta specimens. ALDH1 immunoreactivity was detected with a donkey anti-mouse Alexa Fluor 488 secondary antibody (Figs. 4a, d, g). vWF immunoreactivity was detected, as expected, in endothelial cells lining the chorionic vessels and *decidua basalis* vessels (Figs. 4b, e). In the chorionic villi, the composite image of ALDH1/vWF/DAPI shows overlaps of ALDH1 and vWF immunoreactivity as indicated by the yellow signals (Fig. 4c). The composite image (Fig. 4f) shows some overlap of ALDH1 and vWF immunoreactivity but ALDH1 antigen showed immunoreactivity in the *media* of *decidua basalis* blood vessels (Fig. 4g). FZD-9 immunoreactivity was detected with a goat anti-rabbit Alexa Fluor 568 secondary antibody and showed cytoplasmic staining in cells in the vessel *media* (Fig. 4h). Figure 4i is the composite image showing colocalization of ALDH1 and FZD-9 in the *media* around the *decidua basalis* vessel. The negative control (omission of the primary antibodies) showed no immunoreactivity in the *decidua basalis* vessels (inset in Fig. 4i).

Immunocytochemistry on Primary MSC and MSC Cell Lines

Immunocytochemistry on primary cells (CMSC and DMSC) and cell lines (CMSC29 and DMSC23) was carried out to detect ALDH1 expression at the protein level ($n = 3$). The ALDH1 antigen was detected with a donkey anti-mouse Alexa Fluor 488 secondary antibody and the expression was predominantly cytoplasmic. Figure 5a shows DMSC23 cells stained positively with ALDH1 antibody. In comparison, CMSC29 cells showed weak reactivity with ALDH1 antibody (Fig. 5b). DMSC showed a higher intensity of ALDH1 antibody staining (Fig. 5c) compared to CMSC (Fig. 5d). The negative control was the omission of primary the antibody, which showed no significant staining (inset in Fig. 5d).

Aldefluor Assay

Cells were treated with Aldefluor substrate in the presence of DEAB (ALDH inhibitor) to establish the background fluorescence level; DEAB inhibits the formation of fluorescent products. The fluorescence intensity of cells incubated with the Aldefluor substrate showed a shift in fluorescence that defined the brightly fluorescent ALDH population. A representation of the flow cytometric gating strategy for the Aldefluor assay is shown in Fig. 6a–d. DMSC were incubated with Aldefluor substrate in the presence (Fig. 6a) or absence (Fig. 6b) of DEAB. Similarly, CMSC were stained with Aldefluor in the presence (Fig. 6c) or absence (Fig. 6d) of DEAB. Cells gated in passage P2 (Fig. 6b, d) represent the subpopulation of cells that are positive for ALDH activity, i.e. ALDH^{br} cells.

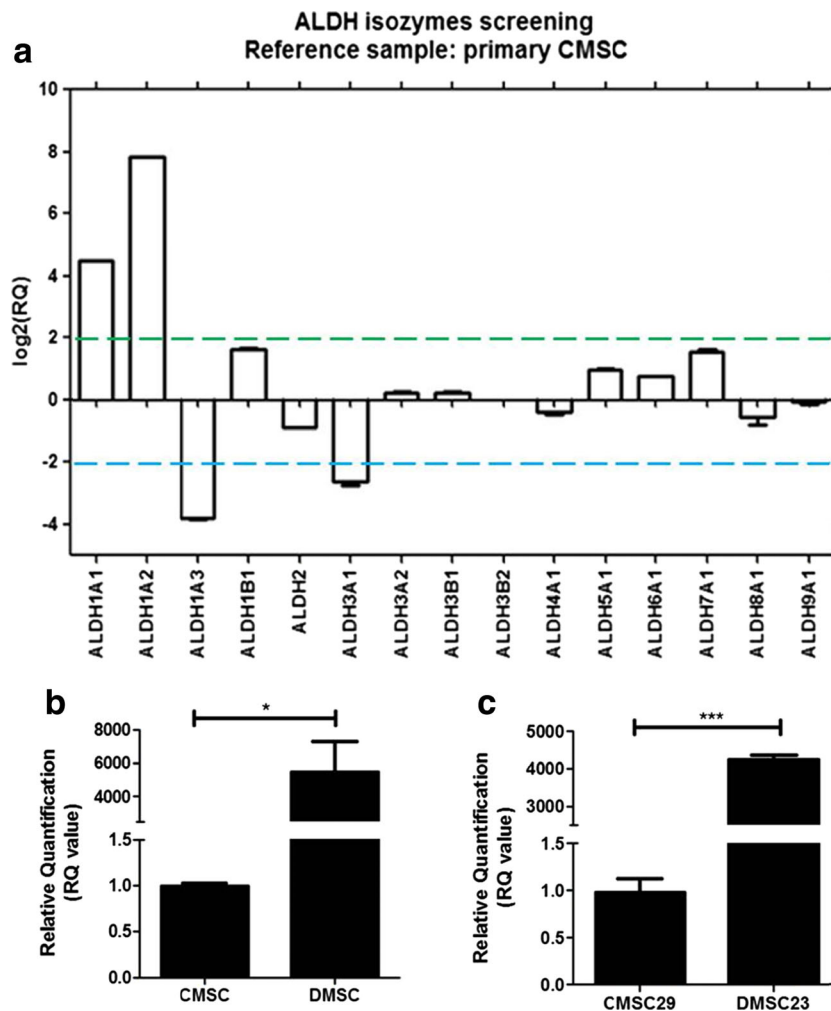


Fig. 3 Real-time RT-PCR. (a) The $\log_2(\text{RQ})$ plot of ALDH isozymes in CMSC and DMSC. For each individual gene, the mRNA level was calculated relative to an endogenous control (18S rRNA is the chosen housekeeping gene). Gene expression was then normalized to the calibrator sample, which was CMSC. The Y-axis shows the $\log_2(\text{RQ})$ values of the particular ALDH isozyme mRNA level. The X-axis shows the ALDH isozymes used in this screening. The green line shows the $\log_2(\text{RQ})$ value at 2-fold increase and the blue line shows the $\log_2(\text{RQ})$ value at 2-fold decrease. Genes that were up-regulated have $\log_2(\text{RQ})$ values >2 and down-regulated genes have $\log_2(\text{RQ})$ values >-2 . Data were presented as mean \pm SEM in duplicate samples. (b) Real-time RT-PCR was performed to determine ALDH1A1 gene mRNA levels relative to the

housekeeping gene 18S rRNA in DMSC and CMSC. The Y-axis shows RQ value of ALDH1A1 mRNA levels in DMSC and CMSC. The reference sample for this experiment was the CMSC sample. Columns represent mean \pm SEM from duplicate samples. Unpaired t-test, $n = 5$ each group, $*p\text{-value} = 0.0274$. (c) Real-time RT-PCR was performed to determine ALDH1A1 gene mRNA levels relative to the housekeeping gene 18S rRNA in DMSC23 and CMSC29 hTERT transformed cell lines. Levels of mRNA were normalized to the reference sample, which were CMSC29 cells. The Y-axis shows RQ value of ALDH1A1 mRNA levels in CMSC29 and DMSC23. Unpaired t-test, $n = 5$ each group, $***p\text{-value} < 0.001$

ALDH Activity in Primary MSCs and MSC Cell Lines

To determine whether differences in ALDH expression were also detectable at the enzyme activity level, ALDH activity was assessed using the Aldefluor assay. The percentage of ALDH^{br} cells and ALDH^{dim} cells in the population was determined. Figure 6e shows DMSC had significantly more ALDH^{br} cells compared with CMSC (DMSC: $19.02 \pm 5.59\%$ vs. CMSC: $0.12 \pm 0.10\%$, $p\text{-value} = 0.007$, $n = 6$, unpaired t-test).

To confirm the Aldefluor assay findings observed in primary MSCs were reflected by MSC cell lines, the Aldefluor

assay was carried out on MSC cell lines. In Fig. 6f, the Aldefluor assay results on the MSC cell lines showed that the DMSC23 cells had a significantly higher percentage of ALDH^{br} cells compared to CMSC29 cells (DMSC23: $20.40 \pm 0.49\%$ vs. CMSC29: $0.27 \pm 0.03\%$, $p\text{-value} < 0.001$, $n = 3$, unpaired t-test).

CFU-F Assay on Sorted Cells

A CFU-F assay was performed to determine whether cell sorting based on ALDH activity would improve colony forming unit ability. CMSC29, which express very low levels

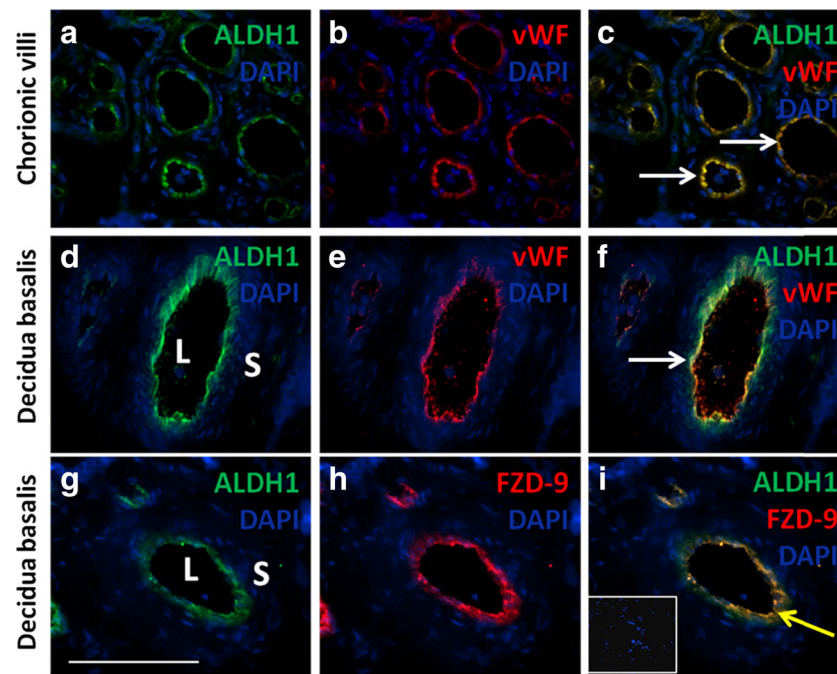


Fig. 4 Multiple immunofluorescence labelling to localize ALDH1 immunoreactivity in the fetal chorionic villi and maternal *decidua basalis* of the placenta. (**a, d, g**) Immunolocalization of ALDH1 using FITC fluorescence. (**b, e**) Immunolocalization of vWF using Cy3 fluorescence. (**c**) Composite ALDH1/vWF/DAPI image in the chorionic villi. White arrows show ALDH1 signal which overlaps the vWF signal. (**f**) Composite ALDH1/vWF/DAPI image around a decidual vessel. White arrows show ALDH1 signal which overlaps the vWF signal. (**g**)

Immunolocalization of ALDH1 using FITC fluorescence. (**h**) Immunolocalization of FZD-9 using Cy3 fluorescence. (**i**) Composite ALDH1/FZD-9/DAPI image around a decidual vessel. Inset shows negative control with the omission of primary antibodies. Yellow arrow shows ALDH1 signal which overlaps the FZD-9 signal. Reactions were carried out on at least 3 different placenta specimens. Cell nuclei were counterstained blue with DAPI in all panels. L: Lumen, S: Stroma. Magnification is 400 \times and scalebar is 100 μ m

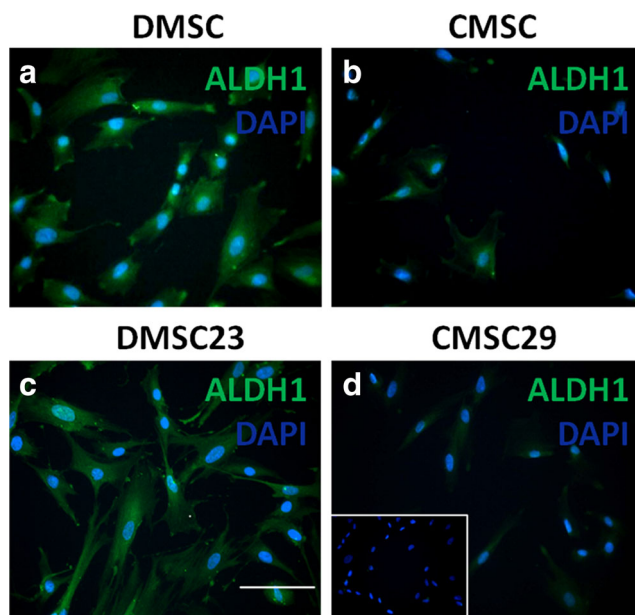


Fig. 5 ALDH1 immunocytochemistry on MSC cell lines (DMSC23 and CMSC29) and primary MSC (DMSC and CMSC). Cells were labelled with ALDH1 antibody (detected with FITC fluorescence) and nuclei were counterstained with DAPI (blue). (**a**) DMSC. (**b**) CMSC. (**c**) DMSC23 cells. (**d**) CMSC29 cells. Inset shows a representative negative control with the omission of primary antibody. Reactions were carried out on at least three independent preparations. Magnification is 200 \times and scalebar is 100 μ m

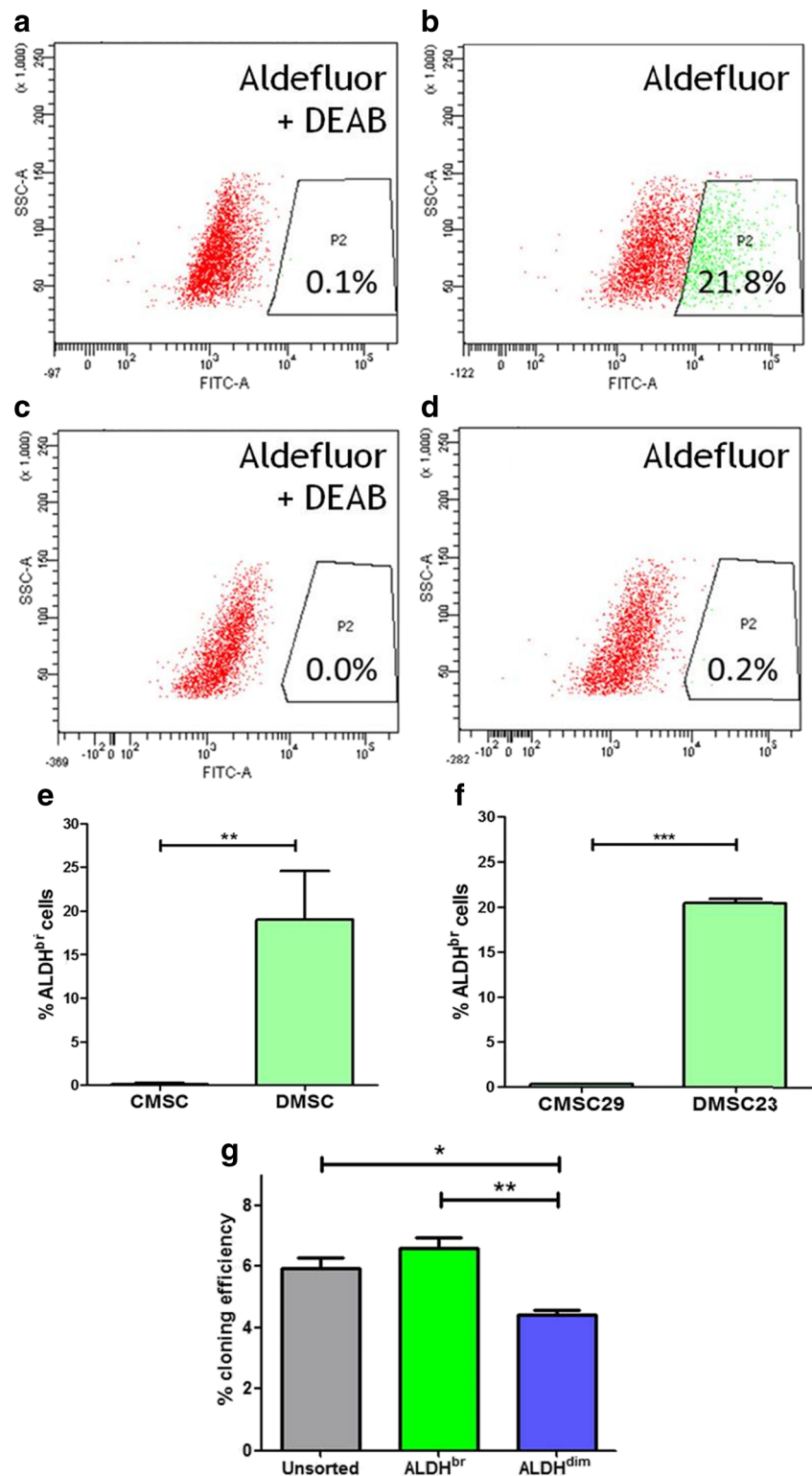
of ALDH enzyme compared with DMSC23, were not assessed.

Purified cell suspensions of unsorted DMSC23, and flow cytometry sorted ALDH^{br} and ALDH^{dim} DMSC23 cells were seeded at densities of 400 cells per well. Approximately 50 % of the cells attached within 24 h of culture. Figure 6g shows the colony forming unit ability of ALDH^{br} DMSC23 cells was significantly higher when compared with ALDH^{dim} DMSC23 cells (Unsorted: 5.92 ± 0.36 %, ALDH^{br}: 6.58 ± 0.36 %, ALDH^{dim}: 4.42 ± 0.17 %, p -value = 0.007, $n = 3$, One-way ANOVA). DMSC were not analysed for their colony forming unit ability due to the large number of cells required for cell sorting (1×10^7 cells) which are difficult to achieve with passaging.

Discussion

In the present work, we show that CMSC and DMSC, which are derived from pregnancy tissues that are exposed to different levels of oxidative stress, expressed different levels of ALDH enzyme. CMSC and DMSC were characterized according to the minimal MSC criteria set by International Society of Cellular Therapy (ISCT) as well as criteria for

Fig. 6 Aldefluor assay in CMSC and DMSC. Representative flow cytometric analysis showing the gating of ALDH^{br} cells, (a) DMSC with added Aldefluor substrate, and the ALDH inhibitor DEAB. (b) DMSC with added Aldefluor substrate. (c) CMSC with added Aldefluor substrate and ALDH inhibitor, DEAB. (d) CMSC with added Aldefluor substrate. The gate (P2 region) for ALDH^{br} cells was determined from the corresponding DEAB panel to establish the baseline level of ALDH expression. The fluorescence intensity of cells incubated with the Aldefluor substrate showed a shift in fluorescence that defined the brightly fluorescent ALDH population called ALDH^{br} cells (X-axis) versus the side scatter (Y-axis). The percentage shown in each panel is the percentage of ALDH^{br} cells in each corresponding sample. (e) The Aldefluor assay was performed on DMSC23 and CMSC29 cells. Unpaired t-test, $n = 6$ each group, $**p$ -value = 0.0070. Columns represent mean \pm SEM. (f) The Aldefluor assay was performed on DMSC23 and CMSC29 cells. The Y-axis shows the percentage of cells with high levels of ALDH (percentage of ALDH^{br} cells). Unpaired t-test, $n = 3$ each group, $***p$ -value < 0.001. (g) The effect of cell sorting on colony forming unit ability. ALDH^{br} and ALDH^{dim} fractions of DMSC23 cells were sorted according to their ALDH activity level using FACS. Unsorted DMSC23 cells and the sorted fractions were then cultured under standard clonogenic assay conditions. The data reflects mean \pm SEM of the % cloning efficiency per 400 cells/well plated in duplicates. One-way ANOVA TEST, $n = 3$ for each group, significant differences were denoted by $**p$ -value < 0.01, $*p$ -value < 0.05



placenta-derived stem cells [35, 36]. Both cell types showed positive expression of MSC markers CD73, CD105, CD90, CD44, CD146, CD166 and lacked the expression of CD45, CD19, and HLA-DR. FISH analysis verified the fetal origin of CMSC and maternal origin of DMSC which were prepared

from a male placenta. Furthermore, both CMSC and DMSC could be differentiated into osteocytes, adipocytes, and chondrocytes consistent with other studies [28–30, 37–39].

The Taqman low density cDNA array was employed to determine the relative mRNA levels of ALDH isozymes in

each of the CMSC and DMSC and then to compare the mRNA levels between CMSC and DMSC. Based on the mRNA levels relative to 18S, ALDH1A1 had the highest level of mRNA with ALDH1B1, and ALDH9A1 also showing high level expression in DMSC. ALDH9A1, ALDH3A2, and ALDH2 were the most highly expressed mRNAs in CMSC. This screening array identified mRNA levels of ALDH1A1 and ALDH1A2 were increased while mRNA levels of ALDH1A3 and ALDH3A1 were decreased in DMSC compared with CMSC. This is the first study to show that ALDH1A1 enzyme was expressed in DMSC and it has the potential to be a functional marker to discriminate between DMSC and CMSC. Immunohistochemistry and DEAB inhibition studies have demonstrated that ALDH1A1 isozyme can also be used as a marker to identify human bone marrow stem cells and breast cancer stem cells [40, 41].

To localize ALDH1 expression in the fetal chorionic villi and maternal *decidua basalis* of human term placenta, multiple immunofluorescence labelling analysis was conducted in combination with vWF and FZD-9 antibodies. In the chorionic villi, ALDH1 immunoreactivity was detected in overlapping with vWF immunoreactivity in endothelial cells. Double immunostaining of ALDH1 and vWF antibodies showed co-localization of the fluorescence signals around the decidual blood vessel and ALDH1 immunoreactivity was also observed in cells in the *tunica intima* of blood vessels in the *decidua basalis*. Double immunostaining of ALDH1 and FZD-9 antibodies showed an overlap of fluorescence signals around the decidual blood vessel. The use of ALDH1 antibody has been extensively demonstrated in various studies to identify normal and malignant human mammary stem cells, normal ovary and ovarian tumors, endometrioid adenocarcinoma cells, and fibroblast-like cells in human fibroids [34, 41–43]. This study employed multi-label immunofluorescence analysis to localize ALDH1 protein expression using the ALDH1-specific antibody. Our previous work showed that MSC markers such as STRO-1, 3G5, α -SMA, and FZD-9 identified vascular MSC niches in the *decidua basalis* and placenta [10, 11]. These studies also reported some overlapping between various MSC markers and vWF expression which are consistent with our observations. Therefore, ALDH1 expression, another possible marker for MSC, co-localized with other MSC markers in the vascular niche. ALDH1 is expressed in the MSC niche in both chorionic villi and *decidua basalis*. Thus, ALDH enzyme activity is potential marker of stem cell identification as demonstrated in several tissue types, including placenta and decidua.

Immunocytochemistry on MSC primary cells utilising an ALDH1 antibody confirmed the findings that the DMSC displayed a higher level of ALDH expression compared to CMSC. The corresponding difference was also found between the DMSC23 and CMSC29 cells. The ALDH1A1 mRNA level was validated by real-time RT-PCR analysis. The

Aldefluor assay results on DMSC and CMSC cells revealed a significant difference in their ALDH enzyme activity, and similarly between DMSC23 and CMSC29 cells. Therefore, in DMSC/DMSC23 there was a significant percentage of the total population of cells with high level ALDH enzyme activity (i.e. ALDH^{br} cells), but this is not the case for CMSC/CMSC29 cells. Overall, the Aldefluor assay result was consistent with ALDH1 immunofluorescence and real-time RT-PCR analysis.

Cell sorting based on ALDH enzyme activity showed that ALDH^{br} DMSC23 cells have a higher clonogenic activity in comparison to ALDH^{dim} DMSC23 cells. Although it is difficult to compare the CFU-F results with previously reported findings because of the different culture protocols, the present findings suggest that colony-forming ability of DMSC23 is at least equal to, or higher than that of BMMSC, adipose MSC, and decidua MSC [44–46]. Our findings are also consistent with other studies demonstrating that sorted ALDH^{br} cells are enriched in their clonogenic activity [47–49].

Based on these findings on MSC cell lines, validation experiments were performed in isolated primary CMSC and DMSC. Immunocytochemistry on primary cells, CMSC and DMSC, utilising an ALDH1 antibody, supported the findings that DMSC displayed a higher level of ALDH expression compared to CMSC. Subsequently, real-time RT-PCR and the Aldefluor assay showed that DMSC has significantly higher ALDH1A1 mRNA levels and ALDH activity compared to CMSC. Immunohistochemistry and DEAB inhibition studies demonstrate that ALDH1A1 isozyme is a major ALDH gene product and ALDH1A1 activity is correlated with Aldefluor assay in human bone marrow stem cells and breast cancer stem cells [40, 41]. We suggest that ALDH1B1 and ALDH9A1 isozymes warrant further investigation into their possible roles in CMSC or DMSC functions.

This study demonstrates that MSC are a heterogeneous population of cells with a subset of cells expressing high level expression of ALDH enzyme, i.e. DMSC consisted of 19.02 ± 5.59 % of ALDH^{br} cells. Other studies have demonstrated that ALDH^{br} cells were detected via Aldefluor assay in cells isolated from various human tissues, for example, 20.1 ± 4.1 % in myoblasts, 34.1 ± 6.2 % in myometrial cells, 6.4 ± 2.9 % in ovarian tumors, 8.2 ± 4.3 % in mammary stem cells, 1.8 ± 1.7 % in umbilical cord MSC, and 0.8 ± 0.2 % in BMMSC [34, 41, 42, 48, 50, 51]. This is consistent with the concept that MSCs are heterogeneous populations of cells and this heterogeneity can affect their potency, safety, tissue specific efficacy, and mechanism of action [52]. Various studies have validated ALDH activity as a marker to enrich stem/progenitor cells in non-hematopoietic organs such as in skeletal muscle, pancreas, colon, brain, prostate, and mammary epithelium [18, 19, 21, 53, 54].

The difference in ALDH expression is likely to be due to the difference in their respective niches. Previously, CMSC

and DMSC were shown to both reside in a vascular niche, but the level of exposure to oxidative stress in *decidua basalis* and chorionic placenta is different. Braekke et al. [15] explored levels of 8-isoprostane, a stable product of lipid peroxidation and a reliable marker of oxidative stress, in cord plasma. They reported that the concentration of 8-isoprostane was significantly higher in plasma from the umbilical vein than from the umbilical artery, suggesting maternal blood is in higher oxidative state compared to fetal blood circulation. Consequently, DMSC are exposed to a high oxidative stress environment due to their close proximity to the maternal blood circulation in the *decidua basalis*. On the other hand, CMSC are located in placental chorionic villi and enveloped by the syncytiotrophoblast layer, exposed exclusively to the fetal blood circulation, which is in a significantly lower oxidative state. Thus, DMSC have a higher percentage of ALDH^{br} cells, which reflects the need to cope with the high oxidative stress environment in the maternal circulation in the *decidua basalis*. The finding that ALDH enzyme expression was significantly different in CMSC and DMSC populations highlights the importance of understanding MSC properties in order to exploit their full potential in regenerative medicine application. For example, DMSC may be better suited to therapeutic application where high oxidative stress environments are encountered such as in cardiovascular disease and tissue inflammation. In future, follow up studies can be undertaken to complement the cell culture work by knocking down ALDH gene in DMSC and test if ALDH gene inactivation causes decreased resistance to oxidative stress. Further research could also utilize both CMSC and DMSC transplantation using in vivo animal model of oxidative stress-related injuries and investigate their effectiveness in restoring oxidative stress conditions. As stated in the introduction, there is strong evidence to support the important role of ALDH enzymes in the MSC resistance to oxidative stress. However, we also acknowledge that other anti-oxidative enzymes and pathways may play important roles, which could be revealed by microarray/proteomics analyses of DMSC, and comparisons with CMSC.

Acknowledgments The authors wish to thank the clinical research midwives, Sue Duggan and Moira Stewart, for patient sample collection at the Royal Women's Hospital. We also thank Dr. Matthew Burton for his advice with flow cytometry gating, Melissa Duggan and Debora Singih for their technical assistance. Financial support was provided by research funding from King Abdullah International Medical Research Centre (Grant No. RC08/114), the Royal Women's Hospital Foundation, and an Australian Stem Cell Centre Postgraduate Scholarship.

References

- Baksh, D., Song, L., & Tuan, R. S. (2004). Adult mesenchymal stem cells: characterization, differentiation, and application in cell and gene therapy. *Journal of Cellular and Molecular Medicine*, 8(3), 301–316.
- da Silva Meirelles, L., Caplan, A. I., & Nardi, N. B. (2008). In search of the in vivo identity of mesenchymal stem cells. *Stem Cells*, 26(9), 2287–2299.
- English, K., French, A., & Wood, K. J. (2010). Mesenchymal stromal cells: facilitators of successful transplantation? *Cell Stem Cell*, 7(4), 431–442.
- Valle-Prieto, A., & Conget, P. A. (2010). Human Mesenchymal Stem Cells Efficiently Manage Oxidative Stress. *Stem Cells and Development*, 19(12), 1885–1893.
- Lodi, D., Iannitti, T., & Palmieri, B. (2011). Stem cells in clinical practice: applications and warnings. *Journal of Experimental & Clinical Cancer Research*, 30(1), 9.
- Mimeault, M., & Batra, S. K. (2006). Concise review: recent advances on the significance of stem cells in tissue regeneration and cancer therapies. *Stem Cells*, 24(11), 2319–2345.
- Peterson, K. M., et al. (2011). Improved survival of mesenchymal stromal cell after hypoxia preconditioning: Role of oxidative stress. *Life Sciences*, 88(1–2), 65–73.
- Rajmakers, M. T. M., et al. (2008). The transient increase of oxidative stress during normal pregnancy is higher and persists after delivery in women with pre-eclampsia. *European Journal of Obstetrics & Gynecology and Reproductive Biology*, 138(1), 39–44.
- Ashok, A., A. Nabil, & Botros, R. (2013). Studies on Women's Health. Oxidative Stress in Applied Basic Research and Clinical Practice ed. N.A. Ashok Agarwal, Botros Rizk, New York: Humana Press.
- Castrechini, N. M., et al. (2010). Mesenchymal stem cells in human placental chorionic villi reside in a vascular Niche. *Placenta*, 31(3), 203–212.
- Kusuma, G.D., et al., (2015). Mesenchymal stem cells reside in a vascular niche in the decidua basalis and are absent in remodelled spiral arterioles. *Placenta*.
- Myatt, L., & Cui, X. (2004). Oxidative stress in the placenta. *Histochemistry and Cell Biology*, 122(4), 369–382.
- Poston, L. and M.T. Rajmakers (2004). Trophoblast oxidative stress, antioxidants and pregnancy outcome—a review. *Placenta*, 25 Suppl A: p. S72-8.
- Jauniaux, E., et al. (2000). Onset of maternal arterial blood flow and placental oxidative stress. A possible factor in human early pregnancy failure. *The American Journal of Pathology*, 157(6), 2111–2122.
- Braekke, K., Harsem, N. K., & Staff, A. C. (2006). Oxidative stress and antioxidant status in fetal circulation in preeclampsia. *Pediatric Research*, 60(5), 560–564.
- Jackson, B., et al. (2011). Update on the aldehyde dehydrogenase gene (*ALDH*) superfamily. *Human Genomics*, 5(4), 283–303.
- Muzio, G., et al. (2012). Aldehyde dehydrogenases and cell proliferation. *Free Radical Biology & Medicine*, 52(4), 735–746.
- Balber, A. E. (2011). Concise review: aldehyde dehydrogenase bright stem and progenitor cell populations from normal tissues: characteristics, activities, and emerging uses in regenerative medicine. *Stem Cells*, 29(4), 570–575.
- Guppy, N., L. Nicholson, and Alison, M. (2011). ABC Transporters, Aldehyde Dehydrogenase, and Adult Stem Cells, in *Adult Stem Cells*, D.G. Phinney, Editor. Humana Press. p. 181-199.
- Douville, J., Beaulieu, R., & Balicki, D. (2008). ALDH1 as a Functional Marker of Cancer Stem and Progenitor Cells. *Stem Cells and Development*, 18(1), 17–26.
- Vauche, K., et al. (2009). Aldehyde dehydrogenase activity identifies a population of human skeletal muscle cells with high myogenic capacities. *Molecular Therapy*, 17(11), 1948–1958.

22. Keller, L. H. (2009). Bone marrow-derived aldehyde dehydrogenase-bright stem and progenitor cells for ischemic repair. *Congestive Heart Failure*, 15(4), 202–206.
23. Chen, Y., et al. (2012). Focus on molecules: *ALDH1A1: from lens and corneal crystallin to stem cell marker*. *Experimental Eye Research*, 102(0): p. 105–106.
24. Sondergaard, C. S., et al. (2010). Human cord blood progenitors with high aldehyde dehydrogenase activity improve vascular density in a model of acute myocardial infarction. *Journal of Translational Medicine*, 8(1), 24.
25. Januchowski, R., Wojtowicz, K., & Zabel, M. (2013). *The role of aldehyde dehydrogenase (ALDH) in cancer drug resistance*. *Biomedicine & Pharmacotherapy*, 67(7), 669–680.
26. Singh, S., et al. *Aldehyde dehydrogenases in cellular responses to oxidative/electrophilic stress*. *Free Radical Biology & Medicine*, 2013. 56(0): p. 89–101.
27. Liu, H., et al. (2014). *A novel combination of homeobox genes is expressed in mesenchymal chorionic stem/stromal cells in first trimester and term pregnancies*. *Reproductive Sciences*, 21(11), 1382–1394.
28. Abumaree, M. H., et al. (2013). Phenotypic and functional characterization of mesenchymal stem cells from chorionic villi of human term placenta. *Stem Cell Reviews*, 9(1), 16–31.
29. Kusuma, G. D., et al. (2015). Ectopic Bone Formation by Mesenchymal Stem Cells Derived from Human Term Placenta and the Decidua. *PLoS One*, 10(10), e0141246.
30. Kusuma, G. D., et al. (2015). Mesenchymal stem cells reside in a vascular niche in the decidua basalis and are absent in remodelled spiral arterioles. *Placenta*, 36(3), 312–321.
31. Qin, S. Q., et al. (2016) Establishment and characterization of fetal and maternal mesenchymal stem/stromal cell lines from the human term placenta. *Placenta*. doi:10.1016/j.placenta.2016.01.018.
32. Livak, K. J., & Schmittgen, T. D. (2001). *Analysis of relative gene expression data using real-time quantitative PCR and the 2^{(-Delta Delta C(T))} Method*. *Methods*, 25(4), 402–408.
33. Moreb, J. S. (2008). Aldehyde dehydrogenase as a marker for stem cells. *Current Stem Cell Research & Therapy*, 3(4), 237–246.
34. Holdsworth-Carson, S. J., et al. (2014). Clonality of smooth muscle and fibroblast cell populations isolated from human fibroid and myometrial tissues. *Molecular Human Reproduction*, 20(3), 250–259.
35. Dominici, M., et al. (2006). Minimal criteria for defining multipotent mesenchymal stromal cells. The International Society for Cellular Therapy position statement. *Cytotherapy*, 8(4), 315–317.
36. Parolini, O., et al. (2008). Concise review: isolation and characterization of cells from human term placenta: outcome of the first international Workshop on Placenta Derived Stem Cells. *Stem Cells*, 26(2), 300–311.
37. Fukuchi, Y., et al. (2004). Human Placenta-Derived Cells Have Mesenchymal Stem/Progenitor Cell Potential. *Stem Cells*, 22(5), 649–658.
38. Nazarov, I., et al. (2012). Multipotent stromal stem cells from human placenta demonstrate high therapeutic potential. *Stem Cells Translational Medicine*, 1(5), 359–372.
39. Zhu, Y., et al. (2014). Placental mesenchymal stem cells of fetal and maternal origins demonstrate different therapeutic potentials. *Stem Cell Research & Therapy*, 5(2), 48.
40. Kastan, M. B., et al. (1990). Direct demonstration of elevated aldehyde dehydrogenase in human hematopoietic progenitor cells. *Blood*, 75(10), 1947–1950.
41. Ginestier, C., et al. (2007). ALDH1 is a marker of normal and malignant human mammary stem cells and a predictor of poor clinical outcome. *Cell Stem Cell*, 1(5), 555–567.
42. Penumatsa, K., et al. (2010) Differential expression of aldehyde dehydrogenase 1a1 (ALDH1) in normal ovary and serous ovarian tumors. *J Ovarian Res.*, 3: p. 28.
43. Rahadiani, N., et al. (2011). *Expression of aldehyde dehydrogenase 1 (ALDH1) in endometrioid adenocarcinoma and its clinical implications*. *Cancer Science*, 102(4), 903–908.
44. Dimitrov, R., et al. (2010). First-trimester human decidua contains a population of mesenchymal stem cells. *Fertility and Sterility*, 93(1), 210–219.
45. Psaltis, P. J., et al. (2010). Enrichment for STRO-1 expression enhances the cardiovascular paracrine activity of human bone marrow-derived mesenchymal cell populations. *Journal of Cellular Physiology*, 223(2), 530–540.
46. Zannettino, A. C., et al. (2008). Multipotential human adipose-derived stromal stem cells exhibit a perivascular phenotype in vitro and in vivo. *Journal of Cellular Physiology*, 214(2), 413–421.
47. Gentry, T., et al. (2007). *Simultaneous isolation of human BM hematopoietic, endothelial and mesenchymal progenitor cells by flow sorting based on aldehyde dehydrogenase activity: implications for cell therapy*. *Cytotherapy*, 9(3), 259–274.
48. Capoccia, B. J., et al. (2009). Revascularization of ischemic limbs after transplantation of human bone marrow cells with high aldehyde dehydrogenase activity. *Blood*, 113(21), 5340–5351.
49. Povsic, T. J., et al. (2009). Aldehyde dehydrogenase activity allows reliable EPC enumeration in stored peripheral blood samples. *Journal of Thrombosis and Thrombolysis*, 28(3), 259–265.
50. Jean, E., et al. (2011). Aldehyde dehydrogenase activity promotes survival of human muscle precursor cells. *Journal of Cellular and Molecular Medicine*, 15(1), 119–133.
51. Nagano, M., et al. (2010). Hypoxia responsive mesenchymal stem cells derived from human umbilical cord blood are effective for bone repair. *Stem Cells and Development*, 19(8), 1195–1210.
52. Watt, S. M., et al. (2013). *The angiogenic properties of mesenchymal stem/stromal cells and their therapeutic potential*. *British Medical Bulletin*, 108, 25–53.
53. Hess, D. A., et al. (2008). Widespread nonhematopoietic tissue distribution by transplanted human progenitor cells with high aldehyde dehydrogenase activity. *Stem Cells*, 26(3), 611c620.
54. Burger, P. E., et al. (2009). *High aldehyde dehydrogenase activity: a novel functional marker of murine prostate stem/progenitor cells*. *Stem Cells*, 27(9), 2220–2228.